Strong electron-phonon coupling of the Fe breathing mode of $LaO_{1-x}F_xFeAs$

Helmut Eschrig*
IFW Dresden, PO Box 270116, D-0111171 Dresden, Germany

The electron-phonon coupling of $LaO_{1-x}F_xFeAs$ is re-investigated on the basis of density functional theory in local density approximation. The implications of the (π,π) nesting of the Fermi surfaces are carefully studied and found to lead to a non-standard electron-phonon coupling of the corresponding Fe in-plane breathing mode, which might make a strong contribution to the high superconducting transition temperature. The semi-metallic behavior of the undoped material is also further illuminated.

PACS numbers: 74.25.Jb,74.25.Kc,74.70.Dd,71.20.-b
Keywords: $FeAsLaO_{1-x}F_x$, superconductor, electron-phonon coupling, Fermi surface nesting

The recently discovered [1] layered superconductor $LaO_{1-x}F_xFeAs$, $0.03 < x < 0.13$, attracts at present considerable interest due to its comparably high critical temperature $T_c \approx 40$K and possibly high upper critical field $H_{c2} \approx 50$Tesla, due to its similarities to the cuprates, and due to many unusual properties. One peculiarity of all density functional based electronic structure calculations [2, 3, 4, 5, 6, 7] is that, although there is strong Fe-3d As-4p covalency resulting in a total width of the corresponding band complex of about 7eV, in a window of about 2.5 eV around and below the Fermi level the electronic states are of nearly pure Fe-3d character (Fig. 1). Mazin *et al.* [5] pointed out that there is a strong Fermi surface (FS) nesting in the undoped material with $q = (\pi, \pi, 0)$ nesting wave vector between the two hole cylinders around the tetragonal axis $\Gamma - Z$ and the two electron cylinders around the axis $M - A$ shifted by q against $\Gamma - Z$ (Fig. 2). This nesting led those and several other authors [6, 7, 8, 9] speculate on an important role of antiferromagnetic correlations with magnetic in-plane superstructure vector (π, π), an apparently well justified scenario. Electron-phonon (e-p) coupling obtained on the basis of density functional perturbation theory [2, 4] yielded only a weak coupling quite not enough to explain the high T_c.

However, as is well known [10, 11] FS nesting also leads to phonon anomalies, and the corresponding e-p coupling may not be correctly described in lowest order perturbation theory which disregards the degeneracy. Moreover, since metallicity and superconductivity take place in the Fe layers of this quasi-two-dimensional tetragonal material only (Fig. 3), an average of linearized e-p coupling over the whole structure might be misleading. In the present text we report results of investigation of these points which might be equally important compared to the magnetic correlations to understand the material. It is indeed found that e-p coupling may be quite strong.

High precision density functional calculations were performed with the local density approximation functional of [12] using the full-potential local-orbital code [13] in the version FPLO7-28 [14] with its default orbital settings. The experimental lattice constants of undoped LaOFeAs, $a = 4.03552$Å, $c = 8.7393$Å, were used,

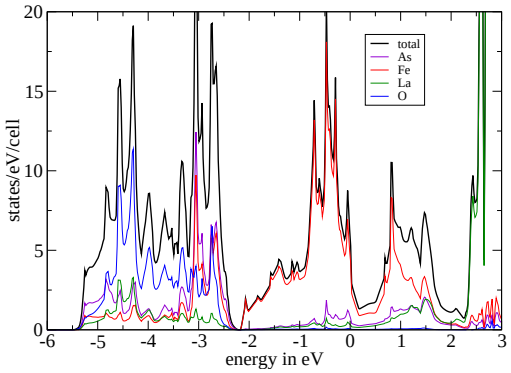

FIG. 1: (color online) Total and component decomposed densities of states of LaOFeAs.

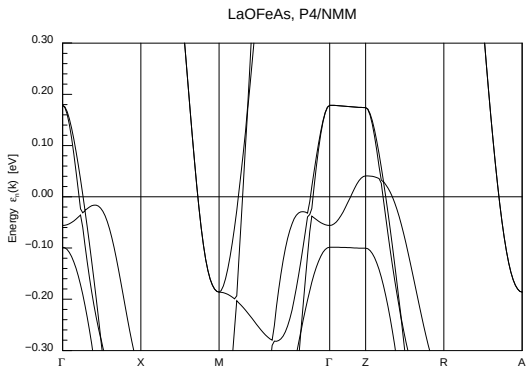

FIG. 2: Bands close to the Fermi level ($\varepsilon_F = 0$) in the P4/nmm zone.

and the two Wyckoff parameters were optimized to be $z_{As} = 0.365$, $z_{La} = 0.1435$.

The phonon mode relevant in this respect is the in-plane breathing mode of the Fe square lattice (checkerboard pattern where every other white square is shrunk, Fig. 4, left part). A static displacement of Fe according

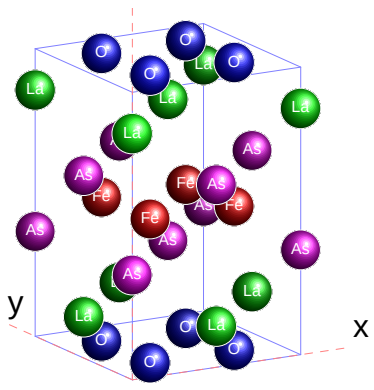

FIG. 3: (color online) The P4mm unit cell (Fe breathing mode) of LaOFeAs.

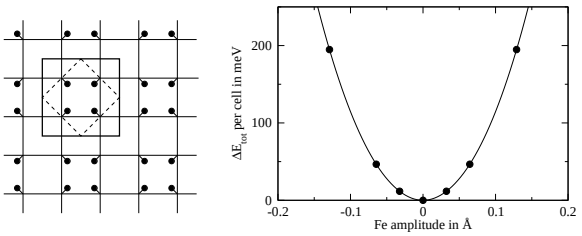

FIG. 4: Left:Displacement pattern of the Fe square lattice for the Fe breathing mode. The P4mm unit cell is shown (thick lines) and the P4/nmm unit cell (dashed lines, its center of inversion for the full structure is half-way between neighboring Fe sites). Right: Total energy per two formula units vs. Fe displacement of the Fe breathing mode.

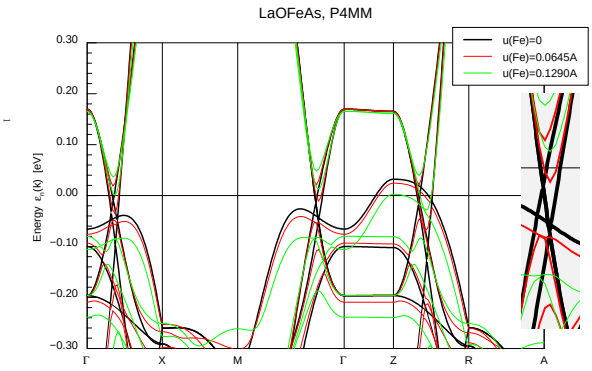

FIG. 5: (color online) Band deformations due to the Fe breathing mode in the P4mm zone. The upward dispersing band on the line $\Gamma - M$ is two-fold degenerate. The inset on the right shows the zoomed detail from the line $M - \Gamma$.

to this breathing mode reduces the P4/nmm symmetry of the lattice to P4mm by doubling the unit cell and removing the inversion from the space group P4/nmm. (The center of inversion was half-way between two neighboring Fe sites.) Doubling the unit cell of the lattice means folding down the unit cell of the reciprocal lattice, the Brillouin zone. The original point $M : \boldsymbol{q} = (\pi, \pi, 0)$ of the P4/nmm lattice (Fig. 2) is folded onto $\Gamma : \boldsymbol{q}' = (0, 0, 0)$ of the P4mm lattice; the folded band structure from Fig. 2 is shown on Fig. 5. For symmetry reasons, at $\boldsymbol{q} = (\pi, \pi, q_3)$ the Fe-mode shown on Fig. 4 could only mix with a corresponding oxygen breathing mode; both are, however, expected to interact only very weakly, and we neglect this mixing. The total energy change due to a static displacement (frozen phonon) is shown on Fig. 4, right part. Despite the FS nesting the mode potential is quite harmonic, the reason for this quadratic dependence on the Fe displacement $u_{\rm Fe}$ is given below. It corresponds to a frequency of $\omega_{\rm Fe} = 29.4$meV in good agreement with the upper limit of the metal mode energies obtained in [2]. Note that there are two equivalent such modes of the Fe atoms as a rotation of the displacement vector by 90° in the left part of Fig. 4 corresponds just to an in-plane shift of the whole P4mm lattice by $(1/2, 0, 0)$ which together with a reflection of the c-axis is a glide symmetry element of the original P4/nmm lattice.

On Fig. 5 the bands corresponding to the undistorted lattice and to two static mode amplitudes, respectively, are shown in the downfolded P4mm zone. The common Fermi level is again $\varepsilon_{\rm F} = 0$. Now, the nesting for $\boldsymbol{q}' = 0$ is seen as band crossings very close to the Fermi level (observe the energy scale of the figure) on the lines $\Gamma - M$ (and $\Gamma - X$) and $Z - R$ (the latter for $q_3' = \pi$; the new point M of the folded zone corresponds to point X on Fig. 2.) From these bands as function of the displacement $u_{\rm Fe}$ of the Fe atoms, deformation potentials are derived. Care is, however, needed since deformation potentials are touchy entities [15]. First of all, they have to be determined from a common Fermi level. In the present case, moreover, reversion of $u_{\rm Fe}$ is equivalent to an in-plane shift of the whole P4mm lattice by $(1, 1, 0)$ which is a lattice vector of the original P4/nmm lattice, and hence changes in band energies $\Delta\varepsilon_{\boldsymbol{k}n}$ must be even in $u_{\rm Fe}$. Consequently, well away from band crossings there is no first order deformation potential, $\Delta\varepsilon_{\boldsymbol{k}n} \sim u_{\rm Fe}^2$. At crossing of folded bands according to the symmetry of the lattice with $u_{\rm Fe} \neq 0$ present (Fig. 5), gaps open with $\Delta\varepsilon_{\rm gap} \sim |u_{\rm Fe}|$. In the vicinity of those crossings one has

$$\Delta\varepsilon_{\boldsymbol{k}n} \approx \pm\sqrt{(v\Delta\boldsymbol{k})^2 + (I_{\rm Fe}u_{\rm Fe})^2} \mp |v\Delta\boldsymbol{k}|, \qquad (1)$$

where v is the average of the two band velocities at the crossing, $\Delta\boldsymbol{k}$ is the deviation from the crossing point, and $I_{\rm Fe}u_{\rm Fe}$ is the deformation potential at the gap:

$$\Delta\varepsilon_{\rm gap} \approx 2I_{\rm Fe}u_{\rm Fe}. \qquad (2)$$

For the displacement corresponding to one phonon per unit cell with energy $\omega_{\rm Fe}$, $\langle u_{\rm Fe}^2 \rangle = (2M_{\rm Fe}\omega_{\rm Fe})^{-1/2}$ one

has $I_{\rm Fe}\langle u^2_{\rm Fe}\rangle^{1/2} \approx 20meV\approx 0.7\omega_{\rm Fe}$. By expanding the square root of (1) for $|v\Delta\boldsymbol{k}| = 20$meV, approximately the position of the FSs of the fluor doped material (at lower doping level compared to Fig. 7, where 12.5 p.c. fluor were considered to limit the computational effort), an FS-averaged e-p coupling constant

$$g = \overline{g_{\boldsymbol{k}n,\boldsymbol{k}'n'}} = \frac{1}{2}\,\frac{I^2_{\rm Fe}\langle u^2_{\rm Fe}\rangle}{20\text{meV}} \approx 10\text{meV} \approx I_{2,\rm Fe}\langle u^2_{\rm Fe}\rangle \quad (3)$$

is obtained, where $I_{2,\rm Fe}$ is the corresponding second order deformation potential. Of course, whenever a phonon mode connects two points on the FS, this gaping with lattice displacement happens. However, normally it happens just for those two points without statistical weight. The peculiarity here is that, as a consequence of the nesting, for one mode it happens in the vicinity of the whole FS in a layer of thickness $\sim\omega_\nu$ in energy (cf. Fig. 6).

In the standard theory the e-p coupling strength $\lambda = Z(0) - 1 = i(\partial\Sigma/\partial\varepsilon)_{\varepsilon=0}$ is obtained from the e-p self-energy

$$\Sigma(\varepsilon) = \sum_{n\nu}\int\frac{d\omega}{2\pi}\int\frac{d^3k}{(2\pi)^3}g^2\frac{2\omega_\nu}{\omega^2+\omega^2_\nu}G_n(\varepsilon-\omega,\boldsymbol{k}) \quad (4)$$

(n being the band index and ν the phonon mode index) by treating the phonon quantities as nearly $\boldsymbol{k}$-independent and using the $\boldsymbol{k}$-integrated electron Green's function

$$\sum_n\int\frac{d^3k}{(2\pi)^3}G_n(\varepsilon-\omega,\boldsymbol{k}) = \\ = N(0)\int_{-\varepsilon_c}^{\varepsilon_c}d\varepsilon_c\frac{1}{i(\varepsilon-\omega)-\varepsilon_c} = \\ = -i\pi N(0)\text{sign}(\varepsilon-\omega) + O(1/\varepsilon_c), \quad (5)$$

where $N(0)$ is the electron density of states (DOS) at the Fermi level, and the high-energy cutoff ε_c is considered negligible small (of the order of Migdal's parameter). Then, the derivative of sign yields a delta function and the ω-integration is readily done yielding $\lambda = \sum_\nu 2N(0)g^2/\omega_\nu$.

In the present case, which is not subject to Migdal's theorem, this approach is not allowed since the renormalized electron Green's functions have a low energy structure at $\eta_c \approx 20$meV, the distance of the gap edges from Fermi level, which causes additional terms in (5). Moreover, Eq. (3) represents a two-phonon vertex (four-leg vertex), and the corresponding contribution to the electron self-energy has two phonon propagators connecting the two vertices and an additional ω-integration in the self-energy, and without the situation with the gaps one would again be left with $\lambda \approx \sum_\nu N(0)g^2/\omega_\nu$, where only g is now the coupling strength (3) of the four-leg vertex, which in the present case is of the same order of magnitude as the usual g of an ordinary three leg vertex. However, due to the gap structure all frequency integrations

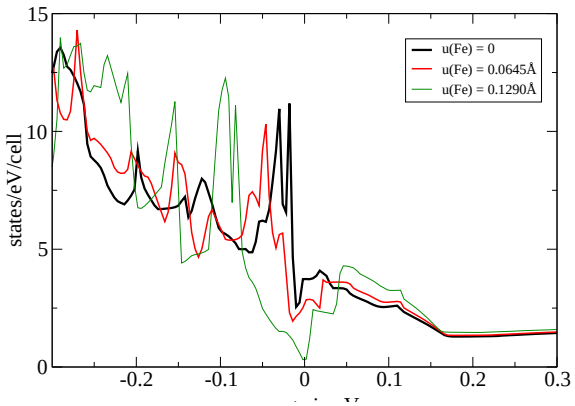

FIG. 6: (color online) Deformation of the total DOS due to the Fe breathing mode (states per two formula units).

are entangled, and resonances of the type $1/(\omega_\nu - \eta_c)$ may appear in the course of self-consistency for G_n [16]. A quantitative theory for this case is complicated and not yet well developed. Non of the approximate assumptions leading to (4) and (5) can be maintained. So far one could only speculate on the magnitude of the effects.

Now, the nesting is considered in more detail. A closer look on Fig. 5 reveals that a displacement $u_{\rm Fe} = 0.0645$Å, which does not much exceed the average displacement of one phonon per mode, already removes two of the four FSs of the in-plane bands (Fe-3d_{xz} and Fe-3d_{yz} orbital character) by opening a gap of about 75meV. Only an electron FS of the shape of a cylindric shell around the tetragonal axis, quite isotropic perpendicular to it, survives (and the hole pocked around point Z of the band of Fe-3d_{z^2} orbital character). Just for illustration the effect of a (not quite realistic) two times larger displacement is also plotted on Fig. 5 for which the material becomes a semi-metal with only two tiny FS pockets, an electron ring and a hole pocket, both around Z. Even slightly larger displacements would make it a true semiconductor. This is reflected in the behavior of the total DOS shown on Fig 6 (where the normalization is for the unit cell of the undistorted P4/nmm structure). One important point is that the nesting is only approximate and, more importantly, that at a given energy the bands which were originally electron or hole bands move in the same direction. Since the band crossings are not exactly at Fermi level and in e-p coupling theory the Fermi level has to be kept fixed [15], the considered e-p coupling is transmitted to all bands and is also transmitted to the band of Fe-3d_{z^2} character. These findings (together with the similar magnetic peculiarities [5]) are capable of explaining many of the unusual electronic properties of the undoped material.

Finally, the effect of fluor doping for oxygen is studied by replacing one of eight oxygen atoms with a fluor atom

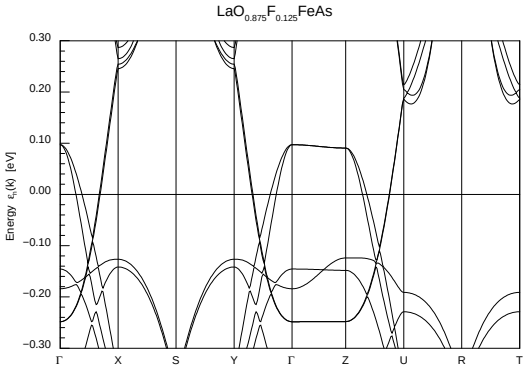

FIG. 7: Bands of $LaO_{0.875}F_{0.125}FeAs$ in the Pmm2 zone.

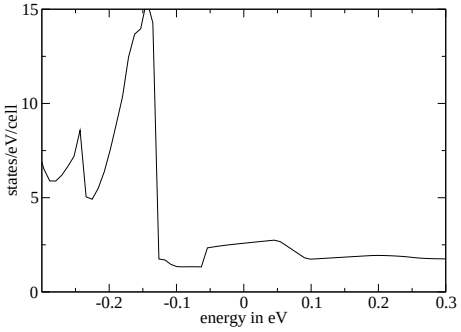

FIG. 8: Total DOS of ordered $LaO_{0.875}F_{0.125}FeAs$ (states per two formula units).

in an ordered way. This reduces the symmetry of the lattice further to the orthorhombic Pmm2 group with a four times larger unit cell, square in plane, compared to the P4/nmm structure. The corresponding bands (again folded, into the Pmm2 zone, which however does not results in new shifts of the FSs which are already close enough to the central line $\Gamma - Z$) and total DOS are shown on Figs. 7 and 8. As can be seen by comparing Figs. 5 and 6 with Figs. 7 and 8, one fluor atom donates just one electron without changing the Fe derived t_{2g}-bands (d_{xz}, d_{yz}) in the vicinity of the Fermi level. Therefore, also no disorder effect of fluor doping is expected in the relevant electronic structure. Moreover, the Fe-$3d_{z^2}$ derived bands, which shift a little bit due to the change of layer charges, are now completely filled (one of them producing the DOS peak at about -150meV), and the corresponding hole pocket around Z has gone, leaving only the four slightly deformed cylindrical FSs, two larger electron cylinders around the $\Gamma - Z$ axis and two smaller hole cylinders around the $M - A$ axis of the original P4/NMM structure (cf. Fig. 2).

In summary, we have shown that the e-p coupling in $LaO_{1-x}F_xFeAs$ is indeed very strong due to the Fe in-plane breathing mode, and this cannot be treated in standard e-p theory of superconductivity. With respect to this breathing mode, the material rather compares with MgB_2, although the details are quite different, and the magnetic couplings already discussed in the literature must also be taken seriously into account. In that respect, the material may have much in common with the cuprates. A principally similar but in detail quite different case is a breathing mode of the copper square lattice in connection with the approximate (π, π)-nesting [16]. It is intriguing hence, whether LaOFeAs could provide some bridge between the other two cases, MgB_2 and the cuprates. The undoped material appears to be a bad metal with a great complexity of very strong couplings, e-p and magnetic. Doping (potentially both electron or hole) moves LaOFeAs away from this messy coupling situation into a still strong coupled but good metallic regime. It is to be expected from former [5] and the present analysis that LaOFeAs will be more symmetric with respect to both electron and hole doping than the cuprates.

Helpful discussion with Klaus Koepernik, Stefan-Ludwig Drechsler, B. Büchner and in particular with M. Eschrig are gratefully acknowledged. I.I. Mazin pointed out to me a substantial error in an earlier version of the paper.

* Electronic address: h.eschrig@ifw-dresden.de; URL: http://www.ifw-dresden.de/institutes/itf/members/helmu

[1] Y. Kamihara, T. Watanabe, M. Hirano, and H. Hosono, J. Am. Chem. Soc. **130**, 3296 (2008).
[2] D. J. Singh and M.-H. Du, cond-mat.supr-con (2008).
[3] G. Xu, W. Ming, Y. Yao, S.-C. Zhang, and Z. Fang, cond-mat.supr-con (2008).
[4] L. Boeri, O. V. Dolgov, and A. A. Golubov, cond-mat.supr-con (2008).
[5] I. I. Mazin, D. J. Singh, M. D. Johannes, and M. H. Du, cond-mat.supr-con (2008).
[6] C. Cao, P. J. Hirschfeld, and H.-P. Cheng, cond-mat.supr-con (2008).
[7] F. Ma and Z.-Y. Lu, cond-mat.supr-con (2008).
[8] K. Kuroki, S. Onari, R. Arita, H. Usui, Y. Tanaka, H. Kontani, and H. Aoki, cond-mat.supr-con (2008).
[9] J. Dong, H. J. Zhang, G. Xu, Z. Li, G. Li, W. Z. Hu, D. Wu, G. F. Chen, X. Dai, J. L. Luo, et al., cond-mat.supr-con (2008).
[10] W. Kohn, Phys. Rev. Lett. **3**, 393 (1959).
[11] A. B. Migdal, Sov. Phys. JETP **34**, 996 (1958).
[12] J. P. Perdew and Y. Wang, Phys. Rev. B **45**, 13244 (1992).
[13] K. Koepernik and H. Eschrig, Phys. Rev. **B59**, 1743 (1999).
[14] http://www.fplo.de.
[15] F. S. Khan and P. B. Allen, Phys. Rev. B **29**, 3341 (1984).
[16] D. M. Newns and C. C. Tsuei, nature physics **3**, 184 (2007).